

## Synthesis, crystal packing and HIV-1 reverse transcriptase studies of 1,1'-(1,3-Phenylene)bis(1H-tetrazole)

Priyanka Singh<sup>a</sup>, M Fátima C Guedes da Silva<sup>b</sup>, Rajesh K Kesharwani<sup>c</sup> & Kafeel Ahmad Siddiqui<sup>a,\*</sup>

<sup>a</sup>Department of Chemistry, National Institute of Technology Raipur, Raipur, Chhattisgarh 492 010, India

<sup>b</sup>Centro de Química Estrutural, Complexo I, Instituto Superior Técnico, Universidade de Lisboa, Av. Rovisco Pais, 1049-001, Lisboa, Portugal

<sup>c</sup>Department of Computer Application, Nehru Gram Bharati (Deemed to be University), Prayagraj, India

\*E-mail: kasiddiqui.chy@nitrr.ac.in

Received 2 August 2022; accepted (revised) 14 March 2023

The compound 1,1'-(1,3-phenylene)bis(1H-tetrazole) (**1**) has been grown while attempting the synthesis of a coordination polymer through metal salt mediated hydrothermal synthesis and their structures have been established by single crystal X-ray diffraction. Pillars involving each of the two independent molecules connected by  $\pi\cdots\pi$  contacts are pivotal in the crystal packing of (**1**). The computational study shows that it might lead molecules for the future drug against HIV.

**Keywords:** C—H $\cdots$ N interaction, Crystal Packing, HIV-1 reverse transcriptase

The creation of molecular crystals is strongly supported by the manifold phenomenon of molecular recognition, which allows molecules to self-organize through non-covalent interactions and ultimately defines the solid state architecture<sup>1,2</sup>. The crystal structures of molecular complexes create opportunities to study how strong and weak hydrogen bonds interact<sup>3</sup>. Definitionally, weak hydrogen bonds do not make a significant contribution to the overall crystal cohesion on an individual basis, their primary significance being their abundance<sup>4-9</sup>. Unlike van der Waals interactions, weak hydrogen bonds (e.g., C—H $\cdots$ N) are the prime example in nature and show attractive forces at relatively long distances, even beyond the theoretical van der Waals contact span. In addition, C—H $\cdots$ X interactions will alter the balance across several choices of stronger bonded networks, thus working as a major "steering force" in solid-state assembly.

Tetrazoles are the ideal ligands for the preparation of the porous frameworks, due to their good networking capabilities<sup>10-14</sup> and they have also proven to be versatile components that form a large number of functional materials<sup>15,16</sup>. A few research groups have shown the importance of C—H $\cdots$ N interactions in coordination and organometallic chemistry<sup>17</sup>. Inorganic chemists have also paid little attention to the effect of  $\pi\cdots\pi$  interactions on the geometry of the coordination complexes<sup>18,19</sup>.

Here we wish to report on the detailed crystal packing analysis of 1,1'-(1,3-phenylene)bis(1H-tetrazole), and their computational evaluation against HIV-1 reverse transcriptase have been studied. We have also observed docking simulation to study the binding affinity of 1,1'-(1,3-phenylene)bis(1H-tetrazole) and compared with other six known compounds and that of the co-crystallized ligand (GW564511) of PDB molecule which in turn elucidate the importance of 1,1'-(1,3-Phenylene) bis(1H-tetrazole) crystal compared to other known anti-viral compounds. Structural formulae of the organic component discussed in this contribution i.e., 1,3-bis(tetrazol-1-yl)benzene is shown in Fig. 1.

### Experimental Details

All chemicals of reagent grade were commercially available and were used without further purification.

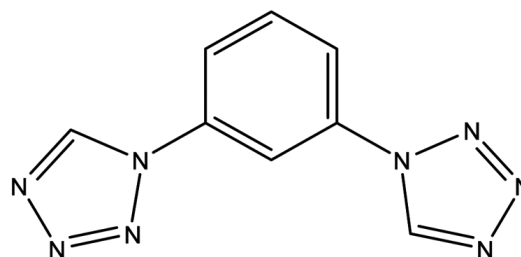


Fig. 1 — Structural formulae of 1,3-bis(tetrazol-1-yl)benzene

### Crystallography

A single crystal of (**1**) with sizes 0.445 x 0.201 x 0.110 mm<sup>3</sup> was mounted on the goniometer head holding the crystal specimen, on a Bruker Apex DUO CCD area detector (fine focus sealed tube fitted with radiation source) with a graphite monochromator and Mo K $\alpha$  radiation ( $\lambda = 0.71073$  Å). The dimensions and intensity data of the unit cells were measured at 150(2) K for (**1**). The structures were solved by direct methods and refined by an F<sup>2</sup>-based complete matrix, with anisotropic thermal parameters for all non-hydrogen atoms using Bruker APEX for data collection and SAINT<sup>20</sup> for cell refining, Bruker SAINT (data reduction), SHELXS-97 (structure solution)<sup>21</sup> SHELXL-2018/3 (structure refining)<sup>22</sup>, and Bruker SHELXTL (molecular graphics) programs<sup>23</sup>. A correction to the absorption of multiple scans (SADABS) has been applied. The hydrogen atoms were included in geometrically determined positions and refined using isotropically (**1**). Lattice parameters and refinement for (**1**) are given in Table 1.

Table 1 — Crystal data and structure refinement details for **1**

Empirical Formula	C <sub>8</sub> H <sub>6</sub> N <sub>8</sub>
Formula weight	214.21
Temperature (K)	150(2)
Wavelength	0.71073
Crystal System	triclinic
Colour	colourless
Space Group	P $\bar{1}$
<i>a</i> (Å)	3.7211(6)
<i>b</i> (Å)	13.719(2)
<i>c</i> (Å)	17.569(3)
$\alpha$ (°)	92.255(9)
$\beta$ (°)	90.994(9)
$\gamma$ (°)	97.748(9)
<i>V</i> (Å <sup>3</sup> )	887.8(3)
<i>Z</i>	4
<i>D</i> <sub>calc</sub> (g/cm <sup>3</sup> )	1.603
Limiting Indices	-3 ≤ <i>h</i> ≤ 4, -17 ≤ <i>k</i> ≤ 17, -21 ≤ <i>l</i> ≤ 21
$\mu$ (mm <sup>-1</sup> )	0.114
<i>F</i> (000)	440
<i>R</i> <sub>int</sub>	0.0365
Theta range for data collection	1.499 to 26.365
Reflections collected	5531
Reflections obs/unique	3375 / 2736
Completeness to theta	93.3%
Absorption correction	multi-scan
Data/restraints/parameters	3375/0/ 289
<i>R</i> ( <i>F</i> ) ( <i>I</i> ≥ 2 $\sigma$ )	0.0615
<i>wR</i> ( <i>F</i> <sup>2</sup> ) (all data)	0.1900
Goodness-of-fit on <i>F</i> <sup>2</sup>	1.137
Largest diff. peak & hole	0.306 & -0.390 e Å <sup>-3</sup>
CCDC No.	1987495

### Crystallization of 1,1'-(1,3-Phenylene)bis(1H-tetrazole) (**1**)

A mixture of CdCl<sub>2</sub> (0.04 g, 0.218 mmol), 1,3-bis(tetrazol-1-yl)benzene (0.015 g, 0.07 mmol), dimethylformamide (4 mL) and distilled water (2 mL) was prepared and sonicated for 15 min, after which, at room temperature, the solution remained undisturbed. After a few days, colorless prism shaped crystals suitable for X-ray diffraction were formed which were isolated by filtration, washed with distilled water, and dried in air. Unfortunately, CdCl<sub>2</sub> did not bind to the synthesized complex and the crystal structure of (**1**) was obtained.

### Results and Discussion

#### Description of Crystal Structure 1,1'-(1,3-Phenylene)bis(1H-tetrazole)(**1**)

Compound crystallized in the triclinic system in space group *P* $\bar{1}$ , its asymmetric unit consists of two crystallographically independent molecules Fig. 2(a); these are easily differentiated by the angles between the least-square plane of the phenylene ring and those of the tetrazoles, assuming values of 2.26 and 6.66° in one molecule, and 8.76 and 24.81° in another. The nitrogen atom of tetrazole of 1,1'-(1,3-Phenylene)bis(1H-tetrazole) as bifurcated donor atom as well as bifurcated acceptor atom which forms dimer involving C—H...N synthons. The hydrogen bonding parameters are listed in Table 2.

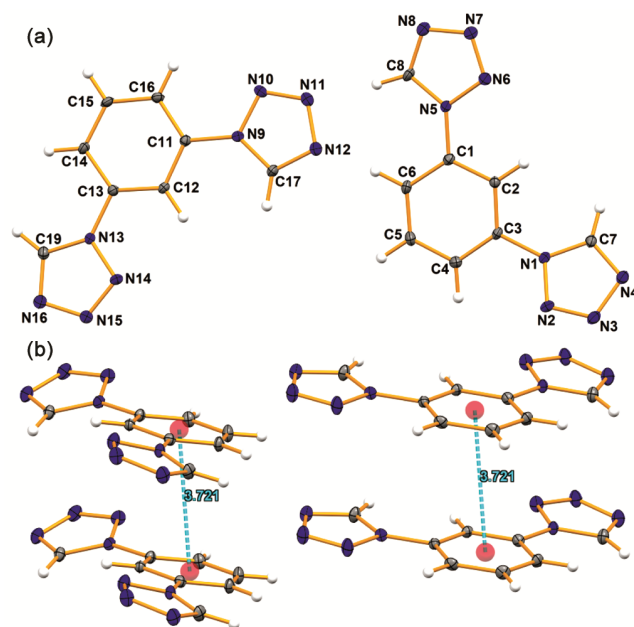


Fig. 2 — (a) Ellipsoid plot (drawn at 30% probability level) of the asymmetric unit of (**1**) with atom labeling scheme and (b) The offset parallel displaced  $\pi \cdots \pi$  interactions with centroid...centroid distances in Å (centroids represented as faded red circles)

Table 2 — C—H...N Hydrogen bonding parameters for **1** (Å) and (°)

D—H...A	d(D—H)	d(H...A)	d(D...A)	<(D—H...A)
C(4)H(4)...N(2)#1	0.950	2.657	3.479	145.06
C(5)H(5)...N(16)#7	0.950	2.687	3.530	148.23
C(6)-H(6)...N(12)#3	0.950	2.746	3.656	160.65
C(7)-H(7)...N(8)#2	0.950	2.590	3.489	169.5
C(8)-H(8)...N(11)#3	0.950	2.614	3.480	151.92
C(8)-H(8)...N(12)#3	0.950	2.393	3.337	172.86
C(14)-H(14)...N(4)#4	0.950	2.582	3.476	157.0
C(16)-H(16)...N(10)#5	0.950	2.584	3.374	140.82
C(17)-H(17)...N(15)#6	0.950	2.335	3.259	164.18
C(19)-H(19)...N(3)#4	0.950	2.465	3.396	166.56
C(19)-H(19)...N(4)#4	0.950	2.718	3.632	161.52

Symmetry transformations used to generate equivalent atoms: #1 -x+2, -y+1, -z+1, #2 -x, -y, -z+1, #3 x-1, y, z, #4 x-1, y, z-1, #5 -x, -y, -z, #6 -x+2, -y+1, -z, #7 -x+1, -y+1, -z

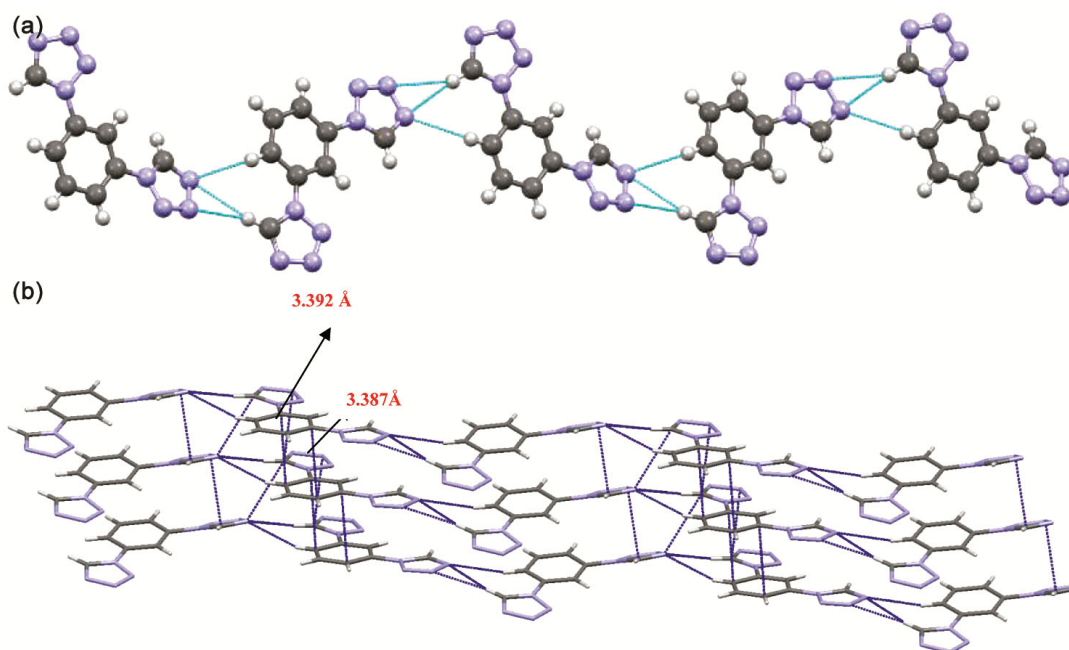


Fig. 3 — (a) View of the crystal lattice along the a-axis showing the 1D zig-zag chain and (b) view of the crystal lattice down crystallographically b axis showing parallel stacked 1-D hydrogen bonded layers through  $\pi \dots \pi$  stacking

The hydrogen bonding through the nearby dimer units between nitrogen atom (N3 & N4) and —C—H group of C19 & C14 carbon of aromatic heterocyclic ring along with c axis results in the formation of 1D zig-zag chain Fig. 3(a). The representation of 1D architecture along the a-axis allows the visualization of a bifurcated intermolecular C—H...N interaction, between the atoms C19—H19...N3(2.465Å) and C19—H19...N4(2.718Å) and N3...H19...N4 angle is 30.04°. Also, the bifurcated intermolecular C—H...N interactions H14 and H19 must be emphasized, C14—H14...N4(2.582Å) and C14—

H19...N4(2.718Å) and H14...N4...H19 angle is 52.24°.

Thus formed 1D layers are parallel stacked along the b axis through  $\pi \dots \pi$  stacking between the benzene rings of the nearby 1D chain of (**1**) and the distance between the two stacking layers was found to be C13—C14=3.392Å and C11—C16=3.387Å Fig. 3(b).

The nearby 1D layers along the c axis are connected by C—H...N hydrogen bond, evolving dimer C4—H4...N2 [(H4...N2=2.657Å), (C4—N2=3.479Å), (C4...H4...N2=145.06°)], C5—

H5...N16 [(H5...N16=2.687Å), (C5...N16=3.530Å), (C5...H5...N16=148.23)] and non-covalent interaction C17—H17...N15 [H17...N15=2.335Å), (C17...N15=3.259Å), (C17...H17...N15=164.18°] in 1<sup>st</sup> layer. While in the 2<sup>nd</sup> layer, the formation of dimer C16—H16...N10 [(H16...N10=2.584Å), (C16—N10=3.374Å), (C16...H16...N10=140.82°)] and presence of bifurcated hydrogen bond between

the atoms C7—H7...N8 (2.590Å) and C7—H7...N7 (2.590Å) and N8...H7...N7 angle is 30.62°. The arrangement goes accordingly, resulting in a 2D hydrogen-bonded network along an *a*-axis Fig. 4(a). The 2D sheets are bonded by  $\pi$ — $\pi$  stacking of the tetrazole rings [C13—C14] and [C11—C16] resulting 3D hydrogen-bonded network along an *a*-axis Fig. 4(b).

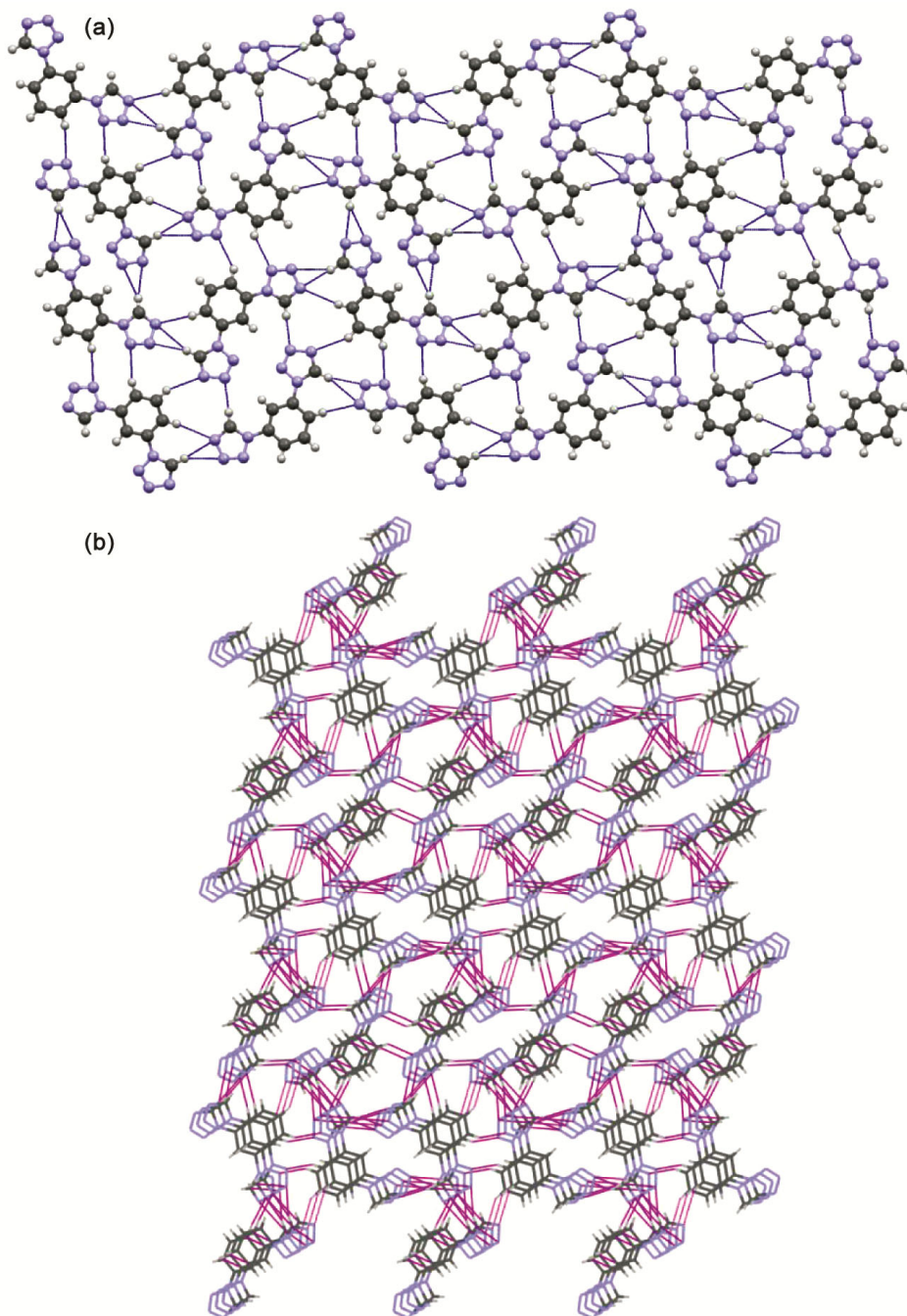


Fig. 4 — (a) view of the crystal lattice along *a*-axis showing 2D network evolving C—H...N synthon and (b) view of a 3D network involving  $\pi$ ... $\pi$  bond

**Docking simulation study against HIV-1 reverse transcriptase**

The 3-dimensional structure of selected potential antiviral drugs including anti-HIV drugs have been downloaded from PubMed<sup>24,25</sup> and Drugbank<sup>26</sup> compound databases. Target protein HIV-1 reverse transcriptase enzyme has been selected for the current study and X-ray structure contains 3-Dimensional information in form of coordinates have been downloaded from protein database (Resolution = 2.20 Å) with GW564511 (co-crystallized ligand) bound at the active site of the receptor (3dlg.pdb)<sup>27</sup>. Ligands have been prepared by using MGL Tool making all the rotatable bonds flexible<sup>28</sup>. Energy minimizations of target protein have been performed by the SPDBV tool using the GROMS 96 force field<sup>29</sup>.

The molecular docking simulation study was carried out using AutoDock Vina to find the activity against the selected HIV target and elucidate the importance of 1,1'-(1,3-Phenylene)bis(1H- tetrazole) crystal compared to other known anti-viral compounds (Abacavir (DB01048), Didanosine (DB00900), Emtricitabine (DB00879), Lamivudine (DB00709), Stavudine (DB00649), Tenofovir alafenamide (DB09299), Tenofovir disoproxil (DB00300), Zidovudine (DB00495) and Rilpivirine (DB08864). The results show the different types of interactions are involved to inhibit the function of the target HIV-1 Reverse Transcriptase enzyme (3dlg.PDB). The docking simulation results show that the binding affinity of 1,1'-(1,3-Phenylene)bis(1H-tetrazole) has stronger binding energies than six known compounds and that of the (co-crystallized ligand (GW564511) of PDB molecule.

The order of binding affinity of docked ligand molecules against the receptor is GW564511 (co-crystallized ligand) > Rilpivirine (DB08864) >

Tenofovir Alafenamide (DB09299) = Zidovudine (DB00495) > 1,1'-(1,3-Phenylene)bis(1H- tetrazole) > Emtricitabine (DB00879) = Stavudine (DB00649) > Abacavir (DB01048) > Didanosine (DB00900), Tenofovir disoproxil (DB00300) and Lamivudine (DB00709) with the range of binding energy being -6.1 to -9.7 kcal/mol. Comparative docking simulation results of selected drugs, PDB bound inhibitor, and chemically synthesized 1,1'-(1,3-phenylene)bis(1H- tetrazole) (**1**) with HIV-1 reverse transcriptase enzyme (3dlg.pdb) using AutoDock Vina<sup>30</sup> (Table 3).

The *in-silico* study results show that the catalytic unit of HIV-1 reverse transcriptase enzyme (3dlg.pdb) active site residues form H-bonds and other interactions (electrophilic and hydrophobic) with ligands to inhibit the normal function of an enzyme. Among the top five docking scores, the synthetic compound is having good binding affinity compared to six known antiviral drugs.

Key residues are always the deciding factor in any enzymatic activity. Table 4 shows that residues of both chains A and B are important for the inhibition of HIV-1 Reverse Transcriptase enzyme activity. It is very clearly shown that key residues of Chain A, Trp 88, Glu 89, Gln 91, and Chain B are Thr 131, Pro 133, Ser 134, Thr 139, and Gly 141 are the most common residues which interact 90-100% docked ligand molecules (Fig. 5a-c). For the enzymatic inhibition, all the major interactions (electronegative, hydrophobic, and hydrogen bonding) are important as depicted by the docked results shown in Table 4, Fig. 5(c). The synthetic compound would lead the molecule for the designing of the potent antiviral drug against HIV disease.

Table 3 — Comparative docking simulation results of selected drugs, PDB bound inhibitor, and chemically synthesized 1,1'-(1,3-Phenylene)bis(1H- tetrazole) (1) with HIV-1 reverse transcriptase enzyme (3dlg.pdb) using AutoDock Vina

S. No.	Ligand Name	Drug Bank Accession Number	(kcal/mol)	No. of H-Bonds
1	GW564511	(Co-crystallized ligand with 3dlg.PDB file )	-9.7	3
2	Rilpivirine	DB08864	-8.8	1
3	Tenofovir Alafenamide	DB09299	-7.5	6
4	Zidovudine_	DB00495	-7.5	8
5	1,1'-(1,3-Phenylene)bis (1H- tetrazole)		-7.4	7
6	Emtricitabine	DB00879	-7.3	3
7	Stavudine	DB00649	-7.3	8
8	Abacavir_	DB01048	-7.2	2
9	Didanosine	DB00900	-7.1	4
10	Tenofovir disoproxil_	DB00300	-6.5	5
11	Lamivudine	DB00709	-6.1	6

Table 4 — Showing active site residues interact with known drugs and chemical synthesized proposed molecules against the target protein, HIV-1 Reverse Transcriptase enzyme

Ligand Name	Interacting residue with chain A of target Protein	Interacting residue with chain B of target Protein
GW564511 (Bound ligand with PDB file)	Trp 88, Glu 89, Gln 91, Leu 92, Gly 93	Lys 22, Gln 23, Trp 24, Pro 25, Asn 57, Thr 131, Pro 133, Ser 134, Thr 139, Pr 140, Gly 141, Arg 143
Rilpivirine (DB08864)	Trp 88, Glu 89, Gln 91, Ile 380, Val 381, Gly 384	Gln 23, Pro 25, Leu 26, Ile 31, Thr 131, Pro 133, Ser 134, Ile 135, Asn 136, Asn 137, Thr 139, Gly 141
1,1'-(1,3-Phenylene)bis(1H-tetrazole)	Trp 88, Glu 89, Gln 91, Leu 92, Gly 93	Lys 22, Gln 23, Trp 24, Pro 25, Asn 57, Thr 131, Pro 133, Ser 134, Asn 137, Thr 139, Pro 140, Gly 141, Arg 143
Abacavir (DB01048)	Trp 88, Glu 89, Gln 91	Gln 23, Trp 24, Pro 25, Leu 26, Ile 31, Asn 57, Thr 131, Pro 133, Ser 134, Asn 136, Asn 137, Thr 139, Pro 140, Gly 141, Ile 380, Val 381
Stavudine (DB00649)	Trp 88, Glu 89, Gln 91	Gln 23, Pro 25, Leu 26, Ile 31, Thr 131, Pro 133, Ser 134, Ile 135, Asn 136, Asn 137, Thr 139, Pro 140, Gly 141, Ile 380, Val 381
Tenofovir Alafenamide (DB09299)	Trp 88, Glu 89, Gln 91, Leu 92, Gly 93, Thr 377, Val 381	Lys 22, Gln 23, Trp 24, Pro 25, Thr 131, Ile 132, Pro 133, Ser 134, Asn 137, Thr 139, Pro 140, Gly 141, Glu 396, Glu 399
Zidovudine (DB00495)	Trp 88, Glu 89, Gln 91, Leu 92, Gly 93, Thr 377, Gln 373	Lys 22, Gln 23, Trp 24, Pro 25, Leu 26, Thr 131, Pro 133, Ser 134, Asn 137, Thr 139, Pro 140, Gly 141, Glu 396, Glu 399, Thr 400
Didanosine (DB00900)	Trp 88, Glu 89, Gln 91, Leu 92, Gly 93, Gln 161	Lys 22, Thr 131, Ile 132, Pro 133, Ser 134, Asn 137, Thr 139, Pro 140, Gly 141
Lamivudine (DB00709)	Trp 88, Glu 89, Val 90, Gln 91, Ala 158, Gln 161, Ser 162, Thr 165, Lys 166	Ile 50, Gly 51, Pro 52, Thr 131, Pro 140, Gly 141, Arg 143
Emtricitabine (DB00879)	Trp 88, Glu 89, Val 90, Gln 91, Leu 92, Gly 93, Ile 94, Val 381	Lys 22, Gln 23, Pro 25, Leu 26, Thr 131, Pro 133, Ser 134, Asn 136, Asn 137, Pro 140, Gly 141
Tenofovir disoproxil (DB00300)	Trp 88, Glu 89, Val 90, Gln 91, Leu 92, Ala 158, Ile 159, Gln 161, Ser 162, Thr 165, Ile 380, Val 381	Lys 22, Gln 23, Trp 24, Pro 25, Leu 26, Thr 131, Pro 133, Ser 134, Ile 135, Asn 136, Asn 137, Thr 139, Pro 140, Gly 141, Ile 142, Arg 143

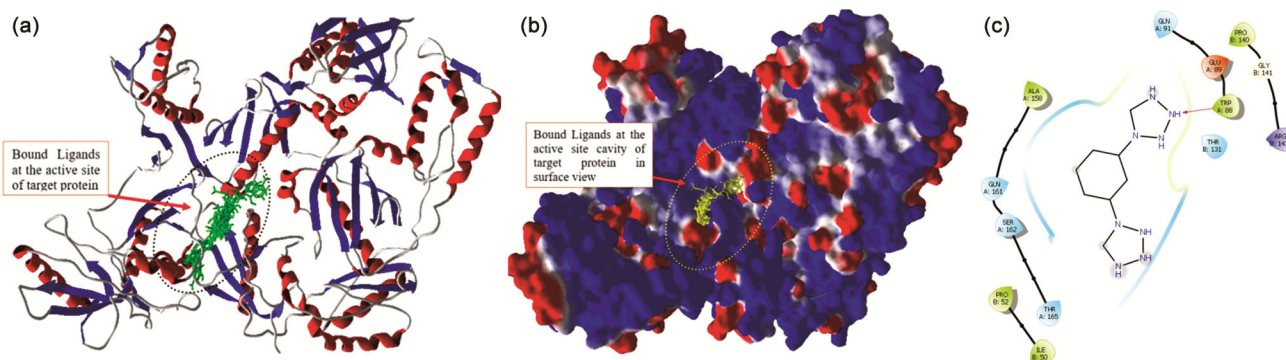


Fig. 5 — (a): Bound confirmation of selected ligands at the active site cavity of target HIV-1 reverse transcriptase enzyme, (b) surface model view of target protein (HIV-1 reverse transcriptase enzyme) with ligands at the active site cavity and (c) active site residues of HIV-1 reverse transcriptase enzyme and bound conformation of chemically synthesized ligand [1,1'-(1,3-Phenylene)bis(1H-tetrazole)] (1)

## Conclusion

A hydrogen bonded 1D chain of 1,1'-(1,3-Phenylene)bis(1H-tetrazole) (**1**) revealed the presence of bifurcated hydrogen bond [(N—H•••N) (C—H•••N)] in the crystal structures. 2D hydrogen bonded framework has been obtained via C—H•••N dimer and C—H•••N bifurcated hydrogen bond

resulting in a 2D framework whereas 3D architecture has been formed via  $\pi\cdots\pi$  stacking in (**1**). Non-covalent bonding (C—H•••N) plays a key role in the creation of organic molecular solid-state structures. Computational evaluation for synthesized compound [1,1'-(1,3-phenylene)bis(1H-tetrazole)] against HIV-1 reverse transcriptase shows that it might lead

molecule for the future drug against HIV and work synergistically with other known drugs after *in vitro* and *in vivo* study.

### Acknowledgment

Dr. Kafeel Ahmad Siddiqui is thankful to the Council of Scientific and Industrial Research, Department of Science and Technology, New Delhi, India, through the sponsored project with order no. 01(2962)/18/EMR-II dated 01/05/2018 to support "Crystal Engineering Research".

### Supplementary Information

Supplementary information is available in the website <http://nopr.niscares.in/handle/123456789/58776>.

### References

- Desiraju G R, Vittal J J & Ramanan A, *Crystal Engineering*, (World Scientific & IISc Press) 2011, p. 232, (<https://doi.org/10.1142/8060>).
- Keith J B, Mettes J A & McClurg R B, *Cryst Growth Des*, 4 (2004) 1009.
- Thaimattam R, Reddy D S, Xue F, Mak T C, Nangia A & Desiraju G R, *J Chem Soc, Perkin Trans II*, (1998) 1783. (<https://doi.org/10.1039/A802452I>)
- Batten S R, Neville S M & Turner D R, *Coordination Polymers: Design, Analysis and Application*, (RSC) 2008.
- Desiraju G R, *Crystal Design: Structure and Function*, (Wiley) 2003.
- Mal K E, Gagnon E, Maris T & Wues J D, *J Am Chem Soc*, 129 (2007) 4306.
- Schmidt G M, *J Pure Appl Chem*, 27 (1971) 647.
- Lehn J-M, *Chem Int Ed Engl*, 29 (1990) 1304.
- Desiraju G R, *Crystal Engineering: The Design of Organic Solids*, (Materials Science Monographs) 1989.
- Cui P, Ren L, Chen Z, Hu H, Zhao B, Shi W & Cheng P, *Inorg Chem*, 51 (2012) 2303.
- Lin Q, Wu T, Zheng ST, Bu X & Feng P, *J Am Chem Soc*, 134 (2012) 784.
- Pachfule P & Banerjee R, *Cryst Growth Des*, 11 (2011) 5176.
- Wang C, Sun L, Lv L, Ni L, Wang S & Yan P, *Inorg Chem Commun*, 18 (2012) 75.
- Kostakis G E, Mondal K C, Anson C E & Powell A K, *Polyhedron*, 29 (2010) 24.
- Sengupta O & Mukherjee P S, *Inorg Chem*, 49 (2010) 8583.
- Szimhardt N, Wurzenberger M H, Beringer A, Daumann L J, & Stierstorfer J, *J Mater Chem*, 5 (2017) 23753.
- Pang W, Zhao J W, Zhao L, Zhang Z K & Zhu S Z, *J Mol Struct*, 1096 (2015) 21.
- Hou J J, Hao Z M & Zhang X M, *Inorg Chim Acta*, 360 (2007) 3959.
- Ghosh R, Rahaman S H, Rosair G M & Ghosh B K, *Inorg Chem Commun*, 10 (2007) 61.
- SAINT Data Reduction Software, Version 6.45, Bruker AXS Inc, (Madison, WI) 2003.
- Sheldrick G M, *Acta Crystallogr*, A64 (2008) 112.
- Uson I & Sheldrick G M, *Acta Crystallogr D*, 74 (2018) 106.
- Sheldrick G M, *SHELXTL. 5.1 ed. Bruker Analytica X-Ray Systems*, (Madison WI) 1997.
- Kim S, Theissen P A & Bolton E E, *Nucleic Acids Res*, 44 (2016) D1202.
- Kesharwani R K, Misra K & Singh D B, *Asian Pac J Trop Med*, 12 (2019) 1.
- Wishart D S, Knox C, Guo A C, Cheng D, Shrivastava S, Tzur D, Gautam B & Hassanali M, *Nucleic Acids Res*, 36 (2008) D901.
- Ren J, Chamberlain P P, Stamp A, Short S A, Weaver K L, Romines K R, Hazen R, Freeman A, Ferris R G, Andrews C W & Boone L, *J Med Chem*, 51 (2008) 5000.
- Singh P, K Kesharwani R, Misra K & I Rizvi S, *J Nad Prod*, 4 (2014) 173.
- Singh D V, Agarwal S, Kesharwani R K & Misra K, *J Mol Model*, 18 (2012) 3903.
- Kesharwani R K, Kumari S, Singh D B & Tripathi S, *Curr Tradit Med*, 6 (2020) 147.